Proceedings of the 21st ICSMGE, Vienna, Austria, 14 – 19 June 2026. Pistrol, Adam & Schweiger (eds.)
Published by: ÖGG, Austrian Society for Geomechanics, Salzburg, Austria, ISBN 978-3-9503898-4-5
https://doi.org/10.53243/ICSMGE2026-475

Surface and soil particles degradation during large deformation sand-steel interface shear tests under different boundary conditions

Jakub Konkol, Marta Moroz, Dominik Maciejewski
Faculty of Civil and Environmental Engineering, Department of Geotechnical and Hydraulic Engineering, Gdansk University of Technology, Poland, jakub.konkol@pg.edu.pl

ABSTRACT: Large deformation shear tests in Bromhead ring shear type apparatus on sand-steel interfaces were carried out. Dry, medium dense Fontainebleau Sand (FS) and two surfaces made of construction steel and of different roughness have been employed. The first interface is brand new steel plate and represents typical material produced in a steel mill. The second one is weathered steel plate covered with natural rust. The sand-steel interfaces were tested under constant normal load (CNL), constant volume (CV) and constant normal stiffness (CNS) conditions, which are typically observed in pile design and research. The surface degradation (wear) was investigated in terms of surface roughness parameters variation such as arithmetical roughness (R_a), and mean peak width (R_{sm}). High initial consolidation stress level equal to 400 kPa was utilized and the displacement level was up to 10 m depending on sand-steel interface type and testing boundary conditions. The CNL interface shear strength is displacement-dependent and can be divided into four stages: (1) maximum interface shear strength, (2) residual stage (up to 100-200 mm), where interface shear strength is constant, (3) abrasion stage (between 100 and 1500 mm) where rust on the steel surface is extensively abraded, and (4) steady stage where particle breakage dominates. The surface degradation results in increase of R_{sm}, but reduction of R_a. The results show that the degradation of FS sand particles can be observed in mesoscale and macroscale. Changes in mesoscale are investigated under microscope and show only small variation in sphericity, but slight increase in roundness with progressing displacements. Changes in macroscale are related to particle breakage. Consequently, it can be demonstrated that the large deformation interface shearing permanently influences the sand and surface properties. The presented preliminary interface shearing tests replicating pile installation shed more light into steel surface and soil degradation mechanisms.

KEYWORDS: Interface shear behavior, large deformations, particles breakage, sand-steel interface, steel surface degradation.

1 INTRODUCTION

Sand-steel interface shear behavior under different boundary conditions has been extensively studied in small-displacement range (e.g. Lashkari 2012; Porcino et al. 2003; Uesugi and Kishida 1986a,b; DeJong and Westgate 2009; Han et al. 2018; Fakharian and Evgin 1997; Vafaei et al. 2021). The studies in large deformation regime are rare and usually conducted under constant normal load (CNL) boundary condition. The CNL boundary condition implies constant load in normal direction on the interface during shearing. While in the past the ring shear (RS) interface testes were focused on silica sands (e.g. Yoshimi and Kishida 1981a,b; Ho et al. 2011), now large deformation RS interface testing on non-cohesive soils is focused on carbonate sands and cyclic loading (e.g. Airey and Kelly 2009; Zhou et al. 2020; Rui et al. 2021). For the purpose of this research only silica sands cases in interface tests will be briefly described. In 1980s sand-steel interface tests under CNL were conducted in ring shear apparatus by Yoshimi and Kishida (1981a,b). They used low carbon structural steel A-36 prepared by wet lapping process with carborodum. However, they made tests only up to the tangential displacement of about 12 mm. Later, a significant contribution to the CNL sand-steel interfaces was made by Imperial College (Klotz 2000; Jardine et al. 2005; Ho 2007; Ho et al. 2011; Barmpopoulos et al. 2010; Yang et al. 2010). For instance, Ho et al. (2011) tested medium dense sands and used air-abraded steel plates of average roughness (R_a) about 4-5 μm. They investigated constant volume interface angle of friction, surface degradation, and particle breakage for different types of sands during shearing up to the 8 m. The RS tests under constant volume (CV) boundary condition were made usually on sands (e.g. Yoshimi and Oh-Oka 1973; Wang et al. 2007; Sassa et al. 2014; Sedano 1998; Sadrekarimi and Olson 2010). However, some examples of sand-steel interfaces can be also found. Probably one the first CV interface tests in RS was made by Yoshimi and Kishida (1981a). More recently, the interface shearing behavior of sand-steel contact in RS under CV (and under cyclic loading) were made by Xu at al. (2025). Very limited research is also related to RS tests under constant normal stiffness (CNS) boundary condition (e.g. Airey and Kelly 2010; Xu et al. 2025). For instance, Airey and Kelly (2010) show lab tests of CNS shearing for silica sands for smooth (R_a=0.4 μm) and very rough (R_a is not provided) sand-steel interfaces up to 50 mm using four different stiffness values.

This research presents sand-steel interface shear behavior under large deformation for two surface types commonly occurring in geotechnical engineering. In contrast to majority of previous research summarized in previous section, interfaces employed in our study are made of construction steel, and their surface is covered with natural rust during controlled weathering process. The main focus is laid on an interface shear strength under different boundary conditions, but the changes in surface topography (variation of average roughness and mean peak width with progressing tangential displacements) and particles shape (roundness and sphericity) are also emphasized.

2 TESTING SETUP

2.1 *Soil*

The soil tested in this research is Fontainebleau sand NE34 (FS) which is pure quartz sand with silica content over 99.7%. The essential soil properties are summarized in Table 1, as more detailed data is provided elsewhere (Andria-Ntoanina et al. 2010).

2.2 *Ring shear apparatus*

Modified Bromhead ring shear apparatus was employed for interface shearing tests. Modification include the sets of PTFE (Polytetrafluoroethylene, commonly known as Teflon) circumferential sealing that prevent soil leakage, which is crucial factor in CV and CNS tests. The ring steel plates are mounted to the top cap and the axial pressure and torque is controlled with combined axial load – torque cell. Vertical displacement is measured by LVDT (Linear Variable Differential Transformer) sensor placed at the top cap.

2.3 *Interfaces*

Two different interfaces were used. Both interfaces are made of construction steel S235. The first one (R2A) is brand new steel ring-shape plate and represents typical material produced in a steel mill. The R_a of R2A interface equals 2.346 µm with R_{sm} = 560 µm. The R2A can be considered as a medium-rough interface. The second interface (R2B) is weathered steel plate covered with rust. The R2B is characterized by R_a = 10.812 µm and R_{sm} = 629 µm. Consequently, the R2B fits the typical values of offshore piles where R_a = 5-10 µm (Jardine and Chow; 1996). Surface profiles with close-up photos on the steel interfaces are presented in Figure 1.

2.4 *Testing program*

Testing program involves two interface types (R2A and R2B), and three boundary conditions (BCs). BCs include CNL, CV, and CNS tests under monotonic rate shearing (20 mm/min). Previous author research on rate-dependency of sand-steel interfaces (Konkol 2025) showed that applied rate does not influence the monotonic shearing of medium dense FS sand under normal stress of 400 kPa. Such an initial consolidation stress was set to reproduce deep soil layers conditions and stress state during pile installation (e.g. Klotz and Coop 2001). CNL tests were conducted up to 10 m while CNS and CV tests were preliminary ones, and the BCs in those tests were maintained only up to the 50 mm of tangential displacements.

Table 1. FS selected properties

Parameter	Symbol	Value	Unit
Soil total unit weight	γ	16.2±0.1	kN/m^3
Critical angle of interface friction	ϕ_c'	31.5±0.5	°
Relative density	D_r	0.62±0.03	-
Average particle size of a soil	D_{50}	210±10	µm
Silica content	SaO_2	99.7	%

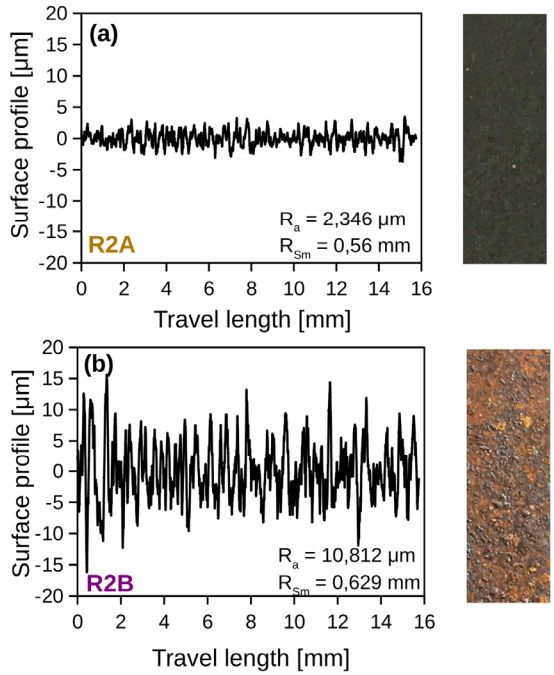

Figure 1. Roughness profiles for (a) R2A interface, and (b) R2B interface (R_A = average roughness; R_{sm} = mean peak width).

3 LARGE DEFORMATION SAND-STEEL INTERFACE TESTS UNDER CNL BOUNDARY CONDITION

3.1 *Interface shear strength*

Interface shear strength (τ_i) under normal stress of 400 kPa, presented in Figure 2a and Figure 2b, shows a complex mechanism of interface shearing. It can be seen, that interface shear strength can be divided into the four regions. The first one is the maximum interface shear strength mobilized at the tangential displacement of about 1-2 mm. Then, the second region (2-100 mm of tangential displacement) of residual shear strength can be distinguished, where τ_i is almost constant. In those two regimes, there is a clear distinction in shear behavior between R2A and R2B. However, between 100 mm and 1500 mm the τ_i for R2A starts to increase which is related with the accumulated abraded steel powder and rust dust in the shear zone (meanwhile, the τ_i for R2B remains at similar level as in previous stage). The steel and rust dusts accumulation results in convergence of τ_i for both R2A and R2B interfaces at about 1.5 m of tangential displacement. Finally, between tangential displacement of 1.5 m and 10 m, the τ_i oscillates and slightly but continuously decreases, which is related with progressing particle breakage and maintained high normal stress level. At the displacement of 10 m, the τ_i for R2A and R2B is almost the same. Dietz and Lings (2006) introduce term "run-in interface friction angle (ϕ'_{ri})" which is related to continuous change during interface shearing. We decided to maintain this nomenclature, as it perfectly captures the interface shear strength behavior. In presented examples, at the end of shearing (tangential displacements about 10 m), ϕ'_{ri} is equal approximately 26.5°, which is slightly lower than CUR (2001) guidelines (where fixed value of 29° is recommended for large displacement regime regardless of displacement level). The obtained ϕ'_{ri} at 10 m is also close to the results presented by Ho et al. (2011), who obtained 27.5° for FS-steel interface shearing at 8 m of tangential displacements and under 400 kPa (initial R_a was about 4.5 µm) and Yang et al. (2010), who obtained ϕ'_{ri} = 24.8° for FS-steel interface shearing at 2 m of tangential displacements (initial R_a was about 3.1 µm making it very close to R2A interface used in this research, normal stress was also equal to 400 kPa). As Yang et al. (2010) research is very close to ours in terms of soil (also FS), steel plates, and BC, a short summary is provided in Table 2 after 1 m of shearing (the only point where direct comparison was possible). It can be concluded, that brand new steel plate (interface R2A), regardless slightly lower roughness, produces slightly higher ϕ'_{ri} than corresponding air-abraded surface in reference research. Remarkable, quite different picture can be seen at displacements of 0.2 m, where R2A returns ϕ'_{ri} = 22.8° in comparison with ϕ'_{ri} = 26.5° in Yang et al. (2010).

Figure 3 presents photos of excavated shearing zone and micrographs of soil grains from this zone after 10 m of shearing. As one can see, there is a lot of rust and steel dirt (or dust) mixed with crushed sand grains located directly in the sand-steel contact zone. The micrographs of the excavated soil grains are very similar for R2A and R2B interfaces. Some of the particles, covered with powder, originated from crushed soil particles and abraded steel. It can be thus hypothesized that for large deformation sand-steel shearing under high normal stress, the steel plate roughness is secondary issue, as it only influences the results up to the 1.5 m of tangential displacement. In that point of view, the CUR (2001) guidelines are correct in fundamental engineering assumption of constant ϕ'_{ri}, for large deformation range, regardless initial surface roughness. However, this research confirms previous findings, that fixed value of 29° is likely to high.

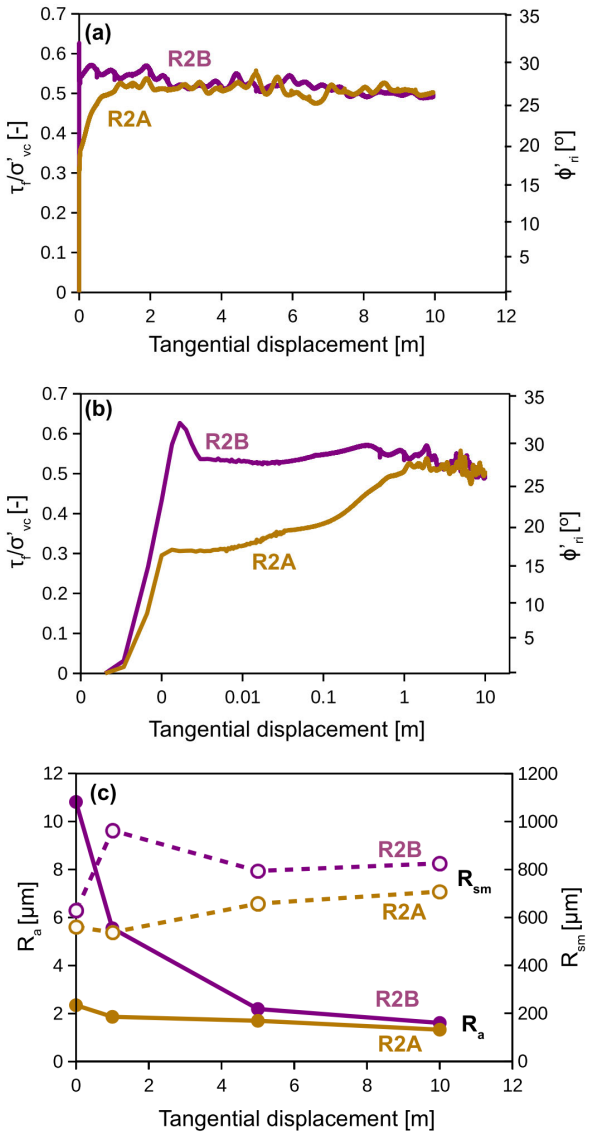

Figure 2. Interface shear strength (τ_f) normalized with consolidation stress (σ'_{vc}) and corresponding run-in interface angle of friction (ϕ'_{ri}) – (a) linear scale, and (b) logarithmic scale; (c) average roughness (R_A) and mean peak width (R_{sm}) change with displacement. Note: data between 50 mm and 10 m was post-processed with Gaussian smoothing algorithm to remove artificial fluctuations and to reduce scatter.

3.2 *Surface degradation (surface wear)*

Two surface characteristics were investigated: (1) R_a which is the arithmetic mean of the absolute values of the profile deviations (also called Center Line Average and abbreviated as R_{CLA}), and (2) R_{sm} which is mean peak width (mean spacing between profile peaks at the center line). Figure 2b shows that accumulated tangential displacements results in steel surface degradation. The most of the roughness decrease can be seen up to the 5 m, and above this value, there is no significant change in any of investigated surface roughness parameters. However, the surface roughness decrease has no significant impact on mobilized interface shear strength. The reason behind this phenomenon is mentioned in previous section – the steel and rust dust gathered at the shear zone, which increase the overall interface shear strength. The comparison between R_a in current research and Yang et al. (2010) is presented in Table 2. The surface degradation is much lower for R2A interface (decrease by approx. 0.5 μm) than for reference interface (decrease by approx. 1 μm). The R_a value after 10 m ($R_{a,10m}$) of shearing is similar for R2A ($R_{a,10m}$=1.327 μm) and R2B ($R_{a,10m}$=1.607 μm). Comparison with reference data after 8 m of shearing – $R_{a,8m}$=1,384 μm in Ho et al. (2011) – shows that our research produces very similar range of surface degradation at large deformation regardless initial roughness and steel surface type.

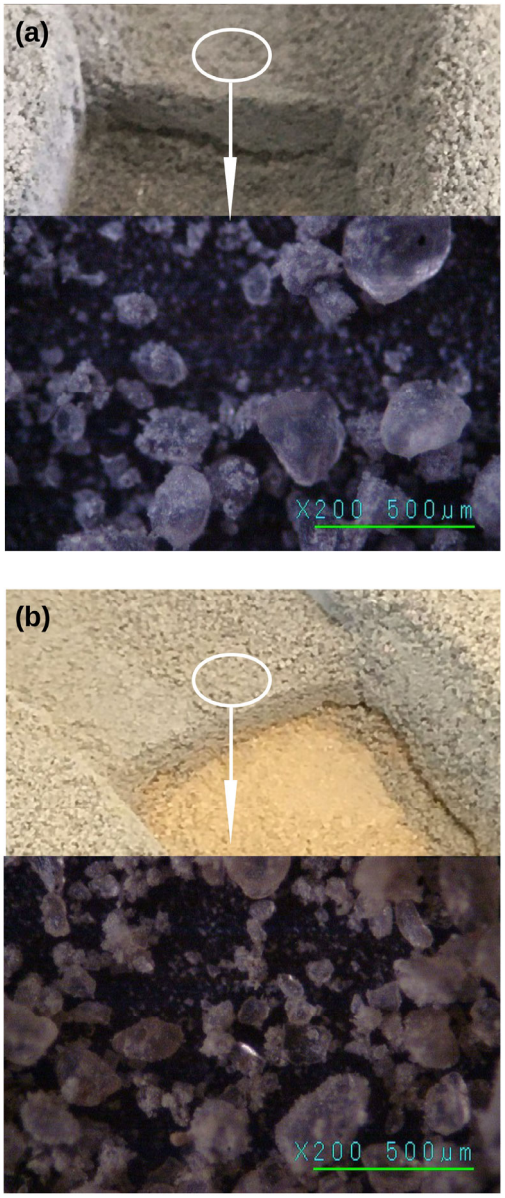

Figure 3. Excavated interface shear zone and optical microscope photos after 10 m of tangential displacement for (a) R2A, and (b) R2B interface.

Table 2. Interface properties after 1m of shearing under CNL mode and 400 kPa. for medium rough interface using FS sand

Parameter	Symbol	Yang et al. (2010)	This research
"Run-in" interface friction angle	ϕ'_{ri}	25.2°	26.6°
Initial average Roughness	$R_{a,0}$	3.072 μm	2.346 μm
Final average Roughness	$R_{a,1m}$	2.022 μm	1.862 μm

3.3 *Soil particles degradation (particle breakage)*

Soil particle degradation can be described in macroscale as a particle size distribution (PSD) change with progressing tangential displacements, and at mesoscale where the soil particle shape factors are changing. The change in PSD for R2A and R2B is shown in Figure 4a, and Figure 4b, respectively. Up to 1 m of tangential displacement, negligible changes can be observed. Then, for amount of fine particles starts to grow, reaching its maximum content after 10 m of displacement. Those outcomes are qualitatively coherent with Yang et al. (2010) and Ho et al. (2011). The analysis of particle breakage in terms of relative breakage B_r, defined by Hardin (1985) as the ratio of total breakage (area between PSD curves before and after the soil has been subjected to loading) to breakage potential (area between the initial particle size distribution curve and a vertical line corresponding to a particle diameter of 0.074 mm), shows slightly higher particle crashing for R2B than for R2A (Figure 5a). The ratio between R2B and R2A is quite constant and equals $B_{r,R2B}=1{,}5B_{r,R2A}$ (where $B_{r,R2A}$ and $B_{r,R2B}$ is relative breakage for R2A and R2B, respectively).

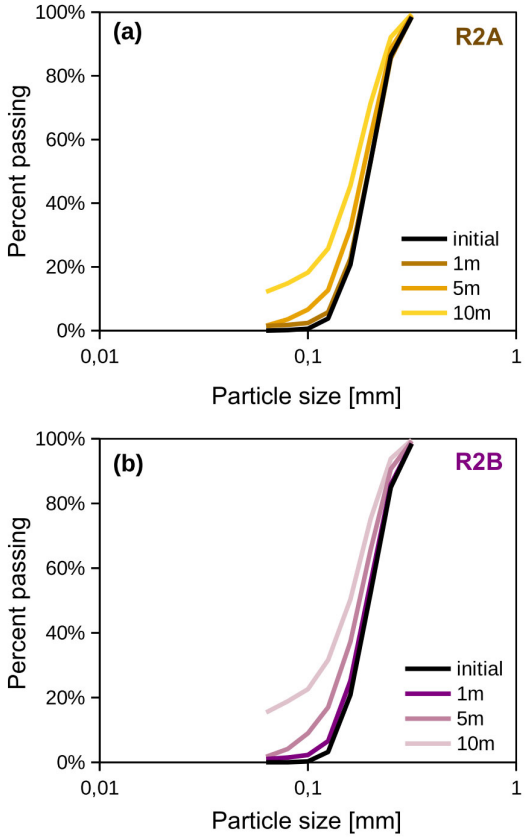

Figure 4. Particle size distribution for (a) R2A interface, and (b) R2B interface.

The next analyzed properties were particle shape characteristics – sphericity and roundness. Sphericity quantifies how closely a particle resembles a perfect sphere while roundness describes degree of edge and corner smoothness of individual grains (Cho et al. 2006). In current research, a custom code developed in the MATLAB environment was used (Zheng and Hryciw 2015). This code analyzes particle images that are derived from micrographs taken under an optical microscope. Those micrographs were firstly imported into AutoCAD, where the contours of individual particles are manually traced. Once the outlines are completed, they are filled internally and subsequently processed using the MATLAB-based code to extract the geometrical characteristics of each particle. The sphericity is defined as circle ratio sphericity (Zheng and Hryciw 2015):

$$S = D_{ins}/D_{cir} \tag{1}$$

while roundness follows traditional Wadells's definition and it is defined as (Cho et al. 2006):

$$R = \frac{\sum r_i N}{r_{max}} \tag{2}$$

where: S = sphericity; D_{ins} = diameter of the largest inscribing circle; D_{cir} = diameter of the smallest circumscribed circle; R = roundness; r_i = radius of curvature at the particle's i-corner, N = number of corners; r_{max} = largest inscribed circle.

Analysis of sphericity and roundness change (Figure 5b) during 10 m of shearing shows no significant variations. The soil particles maintain to be sub-angular and of high sphericity. Noteworthy, soil particles become more spherical and rounded with accumulated tangential displacements up to 5 m. From 5 m and up to 10 m, sphericity remains on similar level, while roundness still increased. The differences between R2A and R2B are not statistically significant. Sphericity and roundness was burdened with standard deviation between 0.05~0.1 making possible only general mechanism to be described. It can be hypothesized that under testing conditions (CNL under 400 kPa) the breakage of soil particles is followed by rolling which produces abraded particles. The interface type contributes only to the magnitude of particle breakage – the higher initial roughness, the higher particle breakage.

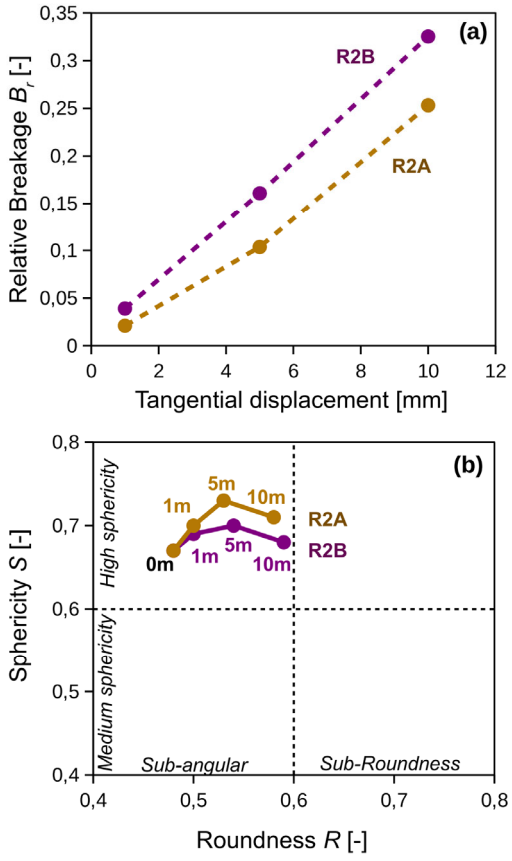

Figure 5. (a) Relative breakage (B_r), and (b) particle shape factors changes during tangential displacement accumulation. Note: S-R classification chart taken from Krumbein and Sloss (1963).

4 LARGE DEFORMATION SAND-STEEL INTERFACE TESTS UNDER CV AND CNS BOUNDARY CONDITIONS

This section presents preliminary tests under CV and CNS conditions. Conduction CNS and CV tests is difficult in RS device due to progressive sealing degradation and soil leakage in consequence. The successful CV and CNS in RS were made up to the tangential displacement between 50 and 200 mm depending on interface type and test setup. The most challenging were CV tests, were even small singular soil grain loss or sealing deformation can transform soil response from dilative to contractive. The comparison between CNL, CV and CNS (k=400 kPa/mm) tests for R2A and R2B interfaces is presented in Figure 6. For slightly rough steel plate (R2A), the CV response is clearly contractive, suggesting soil particles slide on the steel surface. The CNS test falls between CV and CNL. The post-test investigation of the steel surface for R2A shows negligible reduction of the surface roughness (from 1.934 µm to 1.708 µm, and from 2.170 to 1.736 µm for CV, and CNS test, respectively), and only small amount of steel dust mixed with soil particles.

For rough interface (R2B), CV tests shows initial contractive behavior followed by dilative response. However, the effect of high roughness is temporary and degradation of the surface due to high load results in rust removal and change from dilative to contractive behavior. This phenomenon is clearly presented in vertical displacement change (Figure 6b), where sample height is reduce in the initial stage of shearing, then dilatancy acts which results in height increase, and finally, removal of rust switch interface shear behavior form dilative to contractive. It is likely that rust removed during shearing created additional volume (space) in the soil-steel contact zone, which triggered this latter change. The post-test investigation of the surface shows reduction of the roughness for R2B interface (12.398 µm to 9.015µm, and from 11.150 µm to 7.242 µm for CV, and CNS test, respectively), as well as significant amount of rust dust mixed with soil particles. The CNS results show similar behavior to CV test, but of lesser size. There was not significant change in soil particle shape and size detected due to relatively low tangential displacement level.

The CNS and CV interfaces shearing tests can be used for determination of the failure envelopes based on the stress paths. Results shows that interface shear strength for both interfaces can be described by non-linear residual failure envelopes (Figure 6c). However, more tests in this area still needs to be done.

5 CONCLUSIONS

This paper presented large deformation interface shear tests in Bromhead ring shear type apparatus on dry sand-steel interfaces under different boundary conditions. In contrary to majority of interface tests, we incorporated brand new steel plate that represents typical material produced in a steel mill, and steel plate covered with natural rust that is typical material meet at construction site. The following conclusions can be drawn:

1. Interface shear strength is displacement-dependent and can be divided into four stages: (1) maximum interface shear strength related to contractive (R2A) or dilative (R2B) type of interface behavior, (2) residual stage (up to 100 mm), where interface shear strength is constant, (3) abrasion stage (100 to 1500 mm) where rust on the steel surface is extensively abraded, and (4) steady stage where particle breakage dominates.
2. The natural rough steel surfaces (i.e., R2B, $R_a \approx 10$ µm) are likely more vulnerable to roughness degradation than air-abraded steel surfaces. On the other hand, the medium rough steel surface (i.e., R2A, $R_a \approx 3$ µm) is more resistance to surface degradation in initial stage of the shearing and produces lower interface shear strength than air-abraded one. However, at large tangential displacement regime both interfaces return similar interface shear strength to the air-abraded surfaces.
3. The shearing zone is a mixture of crushed soil grains, rust powder and abraded steel dust. The soil crushing is more pronounced for rough interface than for medium rough one, but the relative breakage ratio between those two interfaces is kept constant during whole process of shearing.
4. Soil particle shape factors changes (sphericity and roundness) is similar for both interfaces. The sphericity remains on the same level, but roundness increases with progressing displacement.

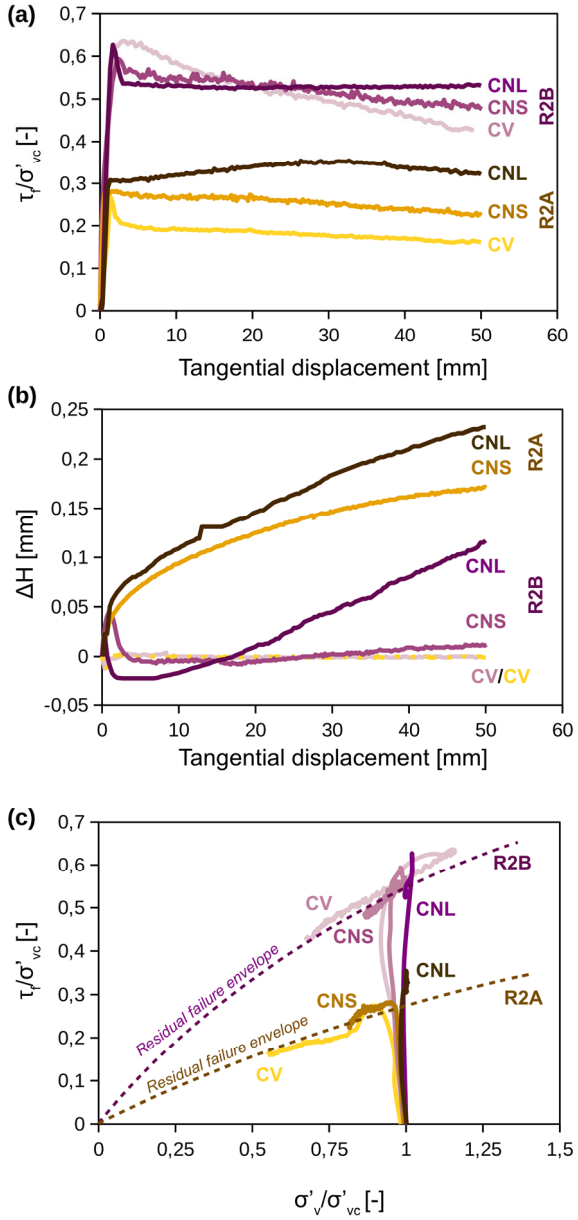

Figure 6. CV and CNS and-steel interface shearing: (a) interface shear strength, (b) sample height change (compression positive), and (c) stress paths. Note: CNL = constant normal load; CV = constant volume, CNS = constant normal stiffness; τ_f = interface shear strength; σ'_{vc} = consolidation stress (400 kPa), σ'_v = effective vertical stress, and ΔH = sample height change.

5. Under CV and CNS boundary conditions the medium rough interface shows clear contractive behavior, while rough interface exhibit change from dilative to contractive behavior due to likely rapid steel surface degradation. Those test revels that interface failure envelope is likely non-linear.

To conclude, the preliminary interface shear tests replicating installation pile performance shed more light into steel surface and soil degradation mechanisms. The findings presented in this paper can be important on post installation analysis of displacement steel piles in on-shore and off-shore applications.

6 ACKNOWLEDGEMENTS

The author are grateful for the financial support provided by National Science Centre. The research presented in this article is supported by project no 2023/51/D/ST8/00786.

7 REFERENCES

Andria-Ntoanina, I., Canou, J., Dupla, J. C. (2010). Caractérisation mécanique du sable de Fontainebleau NE34 à l'appareil triaxial sous cisaillement monotone. CERMES, ENPC/LCPC, Laboratoire Navier–Géotechnique, France.

Airey, D.W., and Kelly, R.B., 2010. Interface behaviours from large diameter ring shear tests. In: *Proceedings of the Research Symposium on Characterization and Behavior of Interfaces* (J.D. Frost, Eds.), 21 September 2008, Atlanta, USA: IOS Press. pp. 7–15.

Barmpopoulos, I.H., Ho, T.Y.K., Jardine, R.J., and Minh, A.N., 2010. The large displacement shear characteristics of granular media against concrete and steel interfaces. In: *Proceedings of the Research Symposium on Characterization and Behavior of Interfaces* (J.D. Frost, Eds.), 21 September 2008, Atlanta, USA: IOS Press. pp. 16–23.

Cho, G.C., Dodds, J., and Santamarina, J.C., 2006. Particle shape effects on packing density, stiffness, and strength: natural and crushed sands. *Journal of Geotechnical and Geoenvironmental engineering*, 132(5), 591-602.

CUR, 2001. *Bearing capacity of steel pipe piles*. Report 2001-8. Gouda, Netherlands: Centre for Civil Engineering Research and Codes.

DeJong, J.T., and Westgate, Z.J. 2009. Role of initial state, material properties, and confinement condition on local and global soil-structure interface behavior. *Journal of Geotechnical and Geoenvironmental Engineering*, 135(11), 1646-1660.

Dietz, M.S., and Lings, M.L. 2006. Postpeak strength of interfaces in a stress-dilatancy framework. *Journal of geotechnical and geoenvironmental engineering*, 132(11), 1474-1484.

Fakharian, K., and Evgin, E., 1997. Cyclic simple-shear behavior of sand-steel interfaces under constant normal stiffness condition. *Journal of Geotechnical and Geoenvironmental Engineering*, 123(12), 1096-1105.

Han, F., Ganju, E., Salgado, R., and Prezzi, M., 2018. Effects of interface roughness, particle geometry, and gradation on the sand–steel interface friction angle. *Journal of Geotechnical and Geoenvironmental Engineering*, 144(12), 04018096.

Hardin, B.O., 1985. Crushing of soil particles. *Journal of geotechnical engineering*, 111(10), 1177-1192.

Ho, T.Y.K. 2007. *Study of the shear behaviour of sand-steel interfaces by ring shear tests*. MSc Thesis, London: Imperial College.

Ho, T.Y.K., Jardine, R.J., and Anh-Minh, N., 2011. Large-displacement interface shear between steel and granular media. *Géotechnique*, 61(3), 221-234.

Jardine, R., Chow, F., Overy, R., and Standing, J., 2005. *ICP design methods for driven piles in sands and clays*. London: Thomas Telford.

Jardine, R.J., and Chow, F.C., 1996. *New design methods for offshore piles*. London: Marine Technology Directorate.

Klotz, U. 2000. *The influence of state on the capacity of driven piles in sands*. PhD Thesis, London: City University.

Klotz, U., and Coop, M.R., 2001. An investigation of the effect of soil state on the capacity of driven piles in sands. *Géotechnique*, 51(9), 733-751.

Konkol, J., 2025. Rate-dependent shear behaviour of silt-steel and sand-steel interfaces. In: *Proceedings of 5th International Symposium on Frontiers in Offshore Geotechnics (ISFOG 2025)*, 9-13 June, Nantes, France: ISSMGE, pp.1-6.

Krumbein, W.C., and Sloss, L.L., 1963. *Stratigraphy and sedimentation*, 2nd Ed., San Francisco: Freeman and Company.

Lashkari, A., 2012. A plasticity model for sand-structure interfaces. *Journal of Central South University*, 19(4), 1098-1108.

Porcino, D., Fioravante, V., Ghionna, V.N., and Pedroni, S., 2003. Interface behavior of sands from constant normal stiffness direct shear tests. *Geotechnical Testing Journal*, 26(3), 289-301.

Rui, S., Wang, L., Guo, Z., Cheng, X., and Wu, B., 2021. Monotonic behavior of interface shear between carbonate sands and steel. *Acta Geotechnica*, 16(1), 167-187.

Sadrekarimi, A., and Olson, S.M., 2010. Particle damage observed in ring shear tests on sands. *Canadian Geotechnical Journal*, 47(5), 497-515.

Sassa, K., Dang, K., He, B., Takara, K., Inoue, K., and Nagai, O., 2014. A new high-stress undrained ring-shear apparatus and its application to the 1792 Unzen–Mayuyama megaslide in Japan. *Landslides*, 11(5), 827-842.

Sedano, J.A.I., 1998. *Constant Volume Ring shear test for sand*. MSc. Thesis, Ottawa: University of Ottawa.

Uesugi, M., and Kishida, H., 1986a. Influential factors of friction between steel and dry sands. *Soils and foundations*, 26(2), 33-46.

Uesugi, M., and Kishida, H., 1986b. Frictional resistance at yield between dry sand and mild steel. *Soils and foundations*, 26(4), 139-149.

Vafaei, N., Fakharian, K., and Sadrekarimi, A., 2021. Sand-sand and sand-steel interface grain-scale behavior under shearing. *Transportation Geotechnics*, 30, 100636.

Wang, G., Sassa, K., Fukuoka, H., and Tada, T., 2007. Experimental study on the shearing behavior of saturated silty soils based on ring-shear tests. *Journal of Geotechnical and Geoenvironmental Engineering*, 133(3), 319-333.

Xu, M., Wang, L., Chen, Z., Zhang, S., and Guo, Z., 2025. Mechanical behavior at silty sand-steel interface undergoing cyclic shearing. *Acta Geotechnica*, 1-21.

Yang, Z.X., Jardine, R.J., Zhu, B.T., Foray, P., and Tsuha, C.D.H.C., 2010. Sand grain crushing and interface shearing during displacement pile installation in sand. Géotechnique, 60(6), 469-482.

Yoshimi, Y., and Oh-Oka, H., 1973. A Ring Torsion Apparatus for Simple Shear Tests. In: *Proceedings of the Eighth International Conference on Soil Mechanics and Foundation Engineering*, 6-11 August, Moscow: USSR National Society for Soil Mechanics and Foundation Engineering, pp. 501-506.

Yoshimi, Y., and Kishida, T., 1981a. Friction Between Sand and Metal Surface. In: *Proceedings of the Tenth International Conference on Soil Mechanics and Foundation Engineering*, 15-19 September, Stockholm: A.A. Balkema, pp. 831-834.

Yoshimi, Y., and Kishida, T., 1981b. A ring torsion apparatus for evaluating friction between soil and metal surfaces. *Geotechnical testing journal*, 4(4), 145-152.

Zheng, J., and Hryciw, R.D., 2015. Traditional soil particle sphericity, roundness and surface roughness by computational geometry. *Géotechnique*, 65(6), 494-506.

Zhou, W., Guo, Z., Wang, L., Li, J., and Rui, S., 2020. Sand-steel interface behaviour under large-displacement and cyclic shear. *Soil Dynamics and Earthquake Engineering*, 138, 106352.